



Shape coexistence in the $N = 19$ neutron-rich nucleus ^{31}Mg explored by β - γ spectroscopy of spin-polarized ^{31}Na



H. Nishibata ^{a,*}, T. Shimoda ^a, A. Odahara ^a, S. Morimoto ^a, S. Kanaya ^a, A. Yagi ^a, H. Kanaoka ^a, M.R. Pearson ^b, C.D.P. Levy ^b, M. Kimura ^c

^a Department of Physics, Osaka University, Osaka 560-0043, Japan

^b TRIUMF, 4004 Wesbrook Mall, Vancouver, BC V6T 2A3, Canada

^c Department of Physics, Hokkaido University, Sapporo 060-0810, Japan

ARTICLE INFO

Article history:

Received 6 January 2017

Received in revised form 23 January 2017

Accepted 24 January 2017

Available online 26 January 2017

Editor: V. Metag

Keywords:

Island of inversion

Shape coexistence

Structure of ^{31}Mg

Spin-polarized ^{31}Na beam

β - γ spectroscopy

ABSTRACT

The structure of excited states in the neutron-rich nucleus ^{31}Mg , which is in the region of the “island of inversion” associated with the neutron magic number $N = 20$, is studied by β - γ spectroscopy of spin-polarized ^{31}Na . Among the ^{31}Mg levels below the one neutron separation energy of 2.3 MeV, the spin values of all five positive-parity levels are unambiguously determined by observing the anisotropic β decay. Two rotational bands with $K^\pi = 1/2^+$ and $1/2^-$ are proposed based on the spins and energies of the levels. Comparison on a level-by-level basis is performed between the experimental results and theoretical calculations by the antisymmetrized molecular dynamics (AMD) plus generator coordinate method (GCM). It is found that various nuclear structures coexist in the low excitation energy region in ^{31}Mg .

© 2017 The Authors. Published by Elsevier B.V. This is an open access article under the CC BY license (<http://creativecommons.org/licenses/by/4.0/>). Funded by SCOAP³.

One of the long-standing subjects of nuclear physics is the shell evolution of nuclei located far from the β -stability line. In particular, neutron-rich Ne, Na, and Mg isotopes with neutron number close to the neutron magic number $N = 20$ have attracted much attention for several decades. In this region of the nuclear chart, it has been suggested by a number of investigations that the ground states of these nuclei are rather deformed, although conventional shell models with a model space of the sd -shell below the $N = 20$ shell gap predicted spherical shapes [1–9]. Typical evidences were such exotic features as anomalous binding energy in Ne [2], Na [3], and Mg [4] isotopes, the low excitation energy of the 2_1^+ states of ^{32}Mg [5], ^{34}Mg [6], ^{30}Ne [7], and the significantly large $B(E2; \text{g.s.} \rightarrow 2_1^+)$ value in ^{32}Mg [8] (the results of subsequent measurements are summarized in Ref. [9]). In the shell model calculations which also take into account the pf -shell, it was suggested that the two-particle–two-hole (2p2h) configurations, which are the results of excitations across the $N = 20$ shell gap, are dominant in the ground state [10–12]. Accordingly, this region in the nuclear chart is known as the “island of inversion” [12]. Such new

features of magic numbers for nuclei far from the β -stability line are reviewed in Ref. [13].

A recent large-scale shell-model calculation [14] predicted that not only deformation in the ground states but also shape coexistence – different shapes coexisting in the low excitation energy region – appear in the excited states, as the result of the competition between the spherical mean field which favors the $0p0h$ configuration and the nuclear correlation which favors the deformed multi-particle–multi-hole (nph) configurations. The coexistence of various structures was also predicted by the theoretical framework of antisymmetrized molecular dynamics (AMD) plus generator coordinate method (GCM), which assumes neither deformation nor mean field [15,16]. The shape coexistence is intensively investigated in several regions of the nuclear chart [17]. The shape coexistence in nuclei is closely related with the quantum phase transition in a finite system, which is under intensive discussion for heavier mass region [18,19].

Up to now, the experimental information on the excited states has been inadequate to address the question of shape coexistence in most nuclei in the $N = 20$ island of inversion. The level structure, such as spin-parity and excitation energy, in the odd-mass nucleus ^{31}Mg is one of the most sensitive probes of shape coexistence, because the last neutron orbit, which governs the

* Corresponding author.

E-mail address: hiroki.nishibata@riken.jp (H. Nishibata).

¹ Present address: RIKEN, Wako, Saitama 351-0198, Japan.

spin-parity of the level, is significantly affected by the degree of nuclear deformation. In this letter, detailed data are presented on the excited states in ^{31}Mg , including spins and parities, obtained in the β decay of spin-polarized ^{31}Na .

After the half-life [5] and the mass [4] of ^{31}Mg were first measured, a long time passed before the magnetic moment [$\mu = -0.88355\mu_N$] and the spin [1/2] of the ground state were measured in the combined measurements of hyperfine structure and β -NMR, and the positive parity was proposed in comparison with the theoretical predictions [20]. It was suggested that the ground state of ^{31}Mg is deformed to a large extent with a nearly pure 2p2h configuration [20], although this nucleus had been considered to be outside of the “island of inversion” [12]. The assignment of $(3/2^+)$ for the first excited state at 0.050 MeV was performed in Ref. [20] based on the $M1$ assignment for the 50-keV γ ray [21] and the $1/2^+$ assignment for the ground state. Experimental information on other excited states of ^{31}Mg is still limited, although many experiments have been performed, such as the β decay [21, 22], the β -delayed one-neutron decay [21–24], the β -delayed two-neutron decay [25], the neutron knockout reaction [26], the proton knockout reaction [27], the Coulomb excitation [28], and the proton resonant elastic scattering [29], as summarized in Refs. [30, 31]. The spins and parities of the ^{31}Mg states have been proposed in some of the experiments; the levels at 0.221 MeV [$(3/2^-)$] [23], 0.461 MeV [$(7/2^-)$] [23], 0.673 MeV [$3/2^+$] [27], 2.015 MeV [$5/2^+$] [27], and 0.945 MeV [$5/2^+$] [28].

In the latest Nuclear Data Sheet [32], 13 levels in ^{31}Mg are listed, including the ground state. Most of their spins and parities are adopted with parenthesis, except for the ground-state spin. In order to discuss the coexistence of various structures predicted by the theoretical calculations [14,15], the detailed properties, including the spins and parities, are needed for the level-by-level basis comparison.

We apply a unique method [33–36] for the spin-parity assignment using the anisotropic β decay of the spin-polarized parent nucleus in the allowed transitions. The angular distribution of β rays is expressed as $W(\theta) \sim 1 + AP \cos \theta$, where A , P and θ are the asymmetry parameter for each β transition, the spin polarization, and the emission angle of β rays with respect to the polarization direction, respectively. The essential point is that the asymmetry parameter A takes very discrete values depending on the spin values of both the parent and the daughter states: In the case of allowed decay of ^{31}Na [$I^\pi = 3/2^+$] [37], the asymmetry parameter equals either -1.0 or -0.4 or $+0.6$ for the possible daughter state in ^{31}Mg with spin-parity of $1/2^+$ or $3/2^+$ or $5/2^+$, respectively. Therefore, from the experimental A value and the allowed nature of the β transitions, accurate spin-parity assignments can be performed.

The AP values are obtained, as follows, by the β -ray counts in coincidence with the γ transition deexciting the ^{31}Mg state which is the daughter state of the β decay. The β -ray counts in the detectors placed at $\theta = 0^\circ$ and $\theta = 180^\circ$ are expressed as $N_0^+ \propto \varepsilon_0(1 + AP)$ and $N_{180}^+ \propto \varepsilon_{180}(1 - AP)$, where ε_0 and ε_{180} are the efficiency of β -ray detection in each detector. The superscript + denotes the polarization direction. If the direction of polarization is reversed by 180 degrees, the β -ray counts are expressed as $N_0^- \propto \varepsilon_0(1 - AP)$ and $N_{180}^- \propto \varepsilon_{180}(1 + AP)$. In order to cancel out the instrumental asymmetry due to detector efficiency, we take the ratios of the four β counts as $R = (N_0^+/N_{180}^+)/(N_0^-/N_{180}^-)$. Then, we obtain the AP value free of the spurious asymmetry as $AP = (\sqrt{R} - 1)/(\sqrt{R} + 1)$. The polarization P is common for all the β transitions and can be evaluated by comparing AP values, as will be discussed later. The experimental asymmetry parameters deduced in this way are affected by the β transitions to the

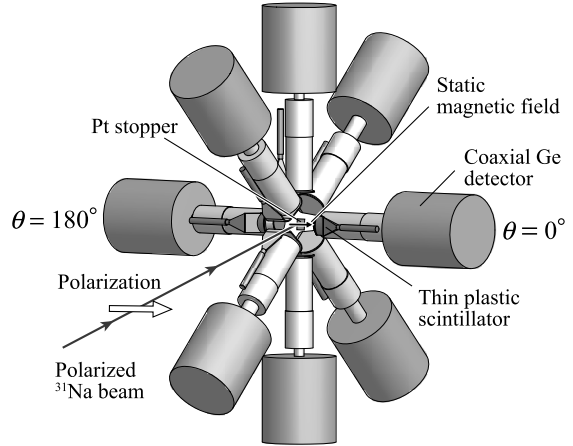


Fig. 1. Experimental setup.

higher states. However, this effect is corrected for by using the intensities of the associated β and γ transitions [35].

The experiment was performed at the Isotope Separator and Accelerator (ISAC) facility in TRIUMF, where highly spin-polarized radioactive Na beams are available. The parent nucleus ^{31}Na ($T_{1/2} = 17.35$ ms [32], $I^\pi = 3/2^+$) was produced in the target fragmentation reaction with the 500-MeV 10 μA proton beam on a uranium carbide target. The $^{31}\text{Na}^+$ ions with an energy of 28 keV were separated by the high resolution mass separator and were delivered to the polarized beam line [38–40]. A high polarization was achieved by simultaneously pumping both atomic ground-state levels with two laser frequencies, and the polarized ^{31}Na beam was transported to the Osaka beam line, where the experimental apparatus for the decay spectroscopy was placed. The direction of the polarization was perpendicular to the beam axis in the horizontal plane.

Fig. 1 shows the experimental setup. The polarized ^{31}Na beam delivered from the left-side was stopped in an annealed Pt foil (20 μm thick) in vacuum. In order to preserve the polarization, a static magnetic field of 0.53 T was applied by a pair of permanent magnets along the polarization direction. The spin orientation was flipped every 100 seconds by changing the direction of the circular polarization of the laser. The β rays and successive γ rays associated with the ^{31}Na β decay were measured by 8 detector-telescopes, each consisting of a high-purity coaxial Ge detector and 1.5 mm thick plastic scintillator(s) in front of the Ge detector. Such a detector configuration was effective in identifying the β rays and the γ rays. The β -decay asymmetry was measured by two telescopes placed at 0° and 180° with respect to the polarization direction. Six other telescopes were placed in a plane perpendicular to the polarization direction. The β ray detection efficiency was $\sim 16\%$ for the left and right telescopes and $\sim 32\%$ for all 8 telescopes. The total efficiency of γ -ray detection was 2.9% at 1.33 MeV. The intensity of ^{31}Na beam at the Pt foil was ~ 200 pps. The accumulated total β - γ coincidence counts were 1.4×10^7 .

Fig. 2 shows the partial γ -ray coincidence spectrum gated by the most intense 50-keV transition which depopulates the 0.050-MeV level in ^{31}Mg . Because of much higher statistics than in the previous works [21,22], many γ -ray peaks are newly observed as transitions in ^{31}Mg . From careful analyses of the two doublets of 892–894 keV and 808–808 keV and the detailed coincidence relations between the γ rays, new levels at 0.942 and 1.436 MeV are found. The proposal of 3.760- and 3.815-MeV levels by Ref. [21] is rejected, because the 3538- and 3710-keV transitions are not found as shown in the inset of Fig. 2. The 1571-keV transition, which was proposed as the transition 3.815 \rightarrow 2.244 [21], is revised as the one 2.244 \rightarrow 0.673.

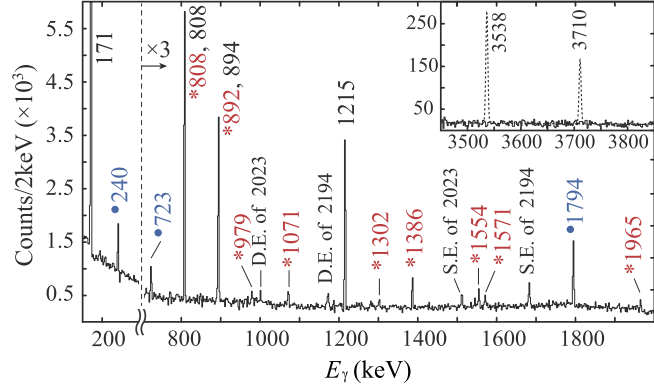


Fig. 2. (Color online.) Partial γ -ray energy spectrum gated by the 50-keV γ ray. The γ peaks labeled with * (shown in red) and • (blue) are those newly found as transitions in ^{31}Mg and those observed in the β decay for the first time, respectively. In the inset, the dashed line shows the expected peaks of the 3538- and 3710-keV γ rays based on the intensities reported in Ref. [21].

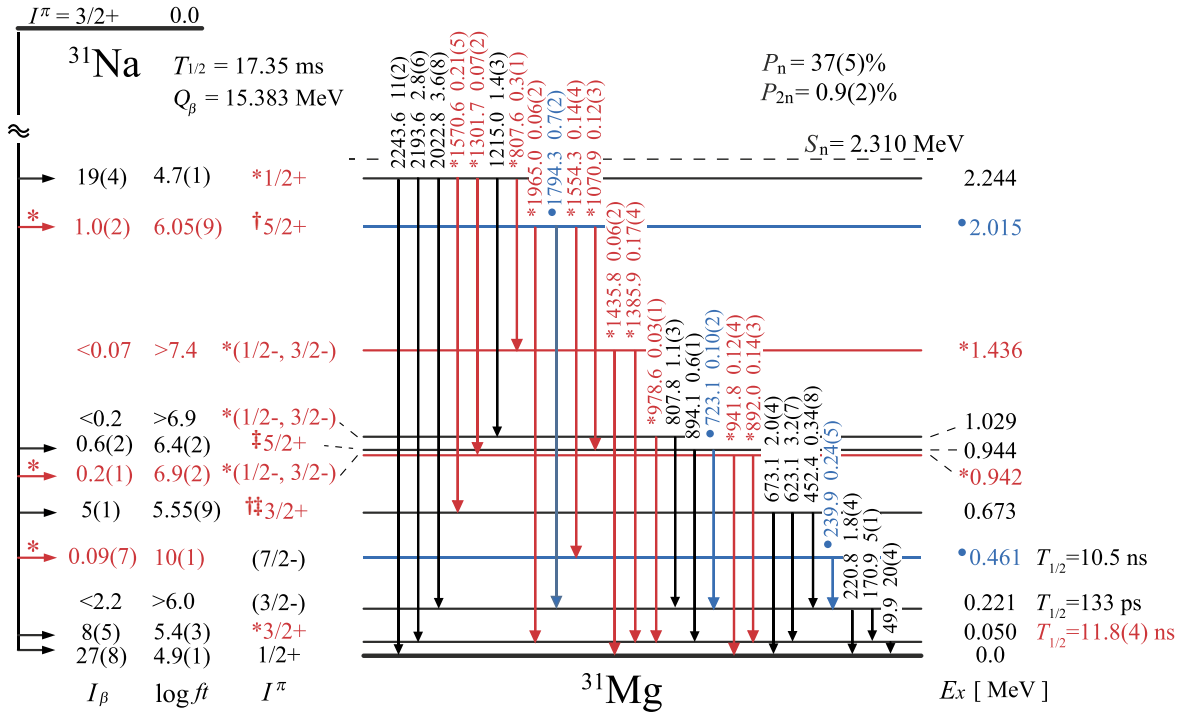


Fig. 3. (Color online.) Revised decay scheme of $^{31}\text{Na} \xrightarrow{\beta} {}^{31}\text{Mg}$ in the present work. The β and γ transitions, levels, and spins and parities labeled with * are newly found in the present work. The spin-parity assignments labeled by \dagger and \ddagger were first proposed by Refs. [27] and [28], respectively, and are confirmed in the present work. The levels and transitions labeled with • are those observed in the β decay for the first time. The β -decay intensity I_β and their $\log ft$ values are also shown (see text).

Before going into the detailed discussion of the level scheme, we show here the revised decay scheme of $^{31}\text{Na} \xrightarrow{\beta} {}^{31}\text{Mg}$ in Fig. 3. The β and γ transitions, levels, and spins and parities shown in red are newly found (labeled with *) or confirmed (\dagger and \ddagger) in the present work. The levels and transitions shown in blue (•) are those observed in the β decay for the first time. It should be noted that 11 γ -ray transitions and 2 levels are found for the first time, and spins of all five positive-parity excited levels are firmly assigned. Furthermore, the spins of three negative-parity states are proposed.

The procedure of the spin-parity assignments is discussed in the following. At first, in order to evaluate the polarization P of the parent nucleus, we focus on two β transitions leading to the levels at 2.244 and 0.673 MeV, whose $\log ft$ values are small and γ feedings from higher levels are negligible. Their experimental AP -values, which are obtained from the β -ray counts gated

by the 2244- and 673-keV γ rays, are $A_{2.244}P = -0.33(1)$ and $A_{0.673}P = -0.11(1)$, respectively. The ratio of A values is deduced as $A_{2.244}P/A_{0.673}P = A_{2.244}/A_{0.673} = 3.0(3)$. Since the A value takes either -1.0 or -0.4 or $+0.6$ for the daughter-state spin-parity of $1/2^+$ or $3/2^+$ or $5/2^+$, respectively, there are 7 possible values for the ratio. Among them the experimental ratio is only consistent with the value of $A(1/2^+)/A(3/2^+) = 2.5$ within two sigma accuracy. Thus, the 2.244- and 0.673-MeV levels are assigned as $1/2^+$ and $3/2^+$, respectively. Then, by using $A_{2.244} = -1.0$ and $A_{0.673} = -0.4$, the polarization P is determined to be $P = 0.32(1)$.

Fig. 4 shows the experimental A values for the levels at 0.050, 0.673, 0.944, 2.015, and 2.244 MeV, which are associated with small $\log ft$ values. It is clearly seen that the experimental values are consistent with one of the expected values, hence the spin-parity assignments are firmly performed as $1/2^+$ for the 2.244-MeV level, $3/2^+$ for the 0.050- and 0.673-MeV levels, and

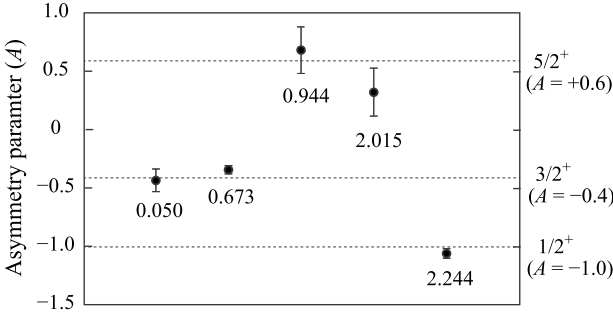


Fig. 4. Experimental asymmetry parameters (A) for the levels at 0.050, 0.673, 0.944, 2.015, and 2.244 MeV in ^{31}Mg . The dashed horizontal lines show the expected A values of -1.0 , -0.4 , and $+0.6$ for $1/2^+$, $3/2^+$, and $5/2^+$, respectively.

$5/2^+$ for the 0.944- and 2.015-MeV levels. It should be emphasized here that the spin-parity of the first excited state at 0.050 MeV, which has not been assigned for a long time, is unambiguously determined to be $3/2^+$ in the present work.

The 0.942-, 1.029-, and 1.436-MeV levels are most likely negative-parity states because of their large $\log ft$ values, which will be discussed later. In order to estimate the spin of the 1.029-MeV level, the γ -transition intensities are compared for the transitions of 1215 keV [$2.244(1/2^+) \rightarrow 1.029$] and the 2244 keV [$2.244(1/2^+) \rightarrow \text{g.s.}(1/2^+)$]. The ratio $I_{1215}/I_{2244} = 0.13(3)$ is consistent with the Weisskopf estimate assuming $E1$ and $M1$ transitions for the former and latter transitions, respectively. Thus the spin-parity of the 1.029-MeV level previously assigned as $(1/2$ to $5/2$, or $7/2^-$) [32] is limited to either $1/2^-$ or $3/2^-$ in the present work. In a similar way, both of the 0.942- and 1.436-MeV levels are assigned as $1/2^-$ or $3/2^-$.

The absolute γ -ray intensities are deduced by referring to the reported 50-keV γ -ray intensity per 100 β decays [$I_\gamma = 19.5(39)$] [21]. The β -decay intensities I_β and their $\log ft$ values are determined by the γ -ray intensities and the neutron-decay probabilities [$P_n = 37(5)\%$ and $P_{2n} = 0.9(2)\%$] [22]. The intensity of the β transition to the ground state is estimated to be $I_\beta = 27(8)$ and $\log ft = 4.9(1)$, which are in good agreement with the reported values [21]. The β transition to the level at 0.461 MeV, whose spin-parity was suggested to be $(7/2^-)$ based on the half-life measurement [23], shows a very large $\log ft$ in the present work, and it is consistent with the first forbidden transition. The half-life for the 0.050-MeV level is measured in the time spectrum between the β ray (plastic scintillator) and the 50-keV γ ray (Ge detector) by using the centroid shift method [41]. The obtained half-life in the present work is $T_{1/2} = 11.8(4)$ ns, the accuracy of which is improved compared to the previous report [$T_{1/2} = 16.0(28)$ ns] [21]. This indicates an $M1$ nature of the 50-keV transition. It is consistent with the spin-parity assignment of $3/2^+$ for the 0.050-MeV level.

In Fig. 5(a), the experimental levels are displayed in three groups, together with the levels not observed in the present work (displayed by dotted lines). The 1.155-MeV level was observed in the proton-knockout reaction from an ^{32}Al beam and the $(7/2^+)$ assignment was proposed by Ref. [27]. The sequence and spacing of the levels in the left group of Fig. 5(a) are consistent with those of a $K^\pi = 1/2^+$ rotational band with a decoupling parameter $a = -0.8$. As for the levels in the middle group of Fig. 5(a), the 1.390-MeV level was observed in the β -delayed neutron decay of ^{32}Na , and the $\geq 3/2^-$ assignment was proposed by Ref. [21]. We propose here an assignment of $11/2^-$ tentatively, so that the levels in the middle group are in good agreement with members of a $K^\pi = 1/2^-$ rotational band with a decoupling parameter $a = -4.5$. Note that similar bands of $K^\pi = 1/2^+$ and $1/2^-$

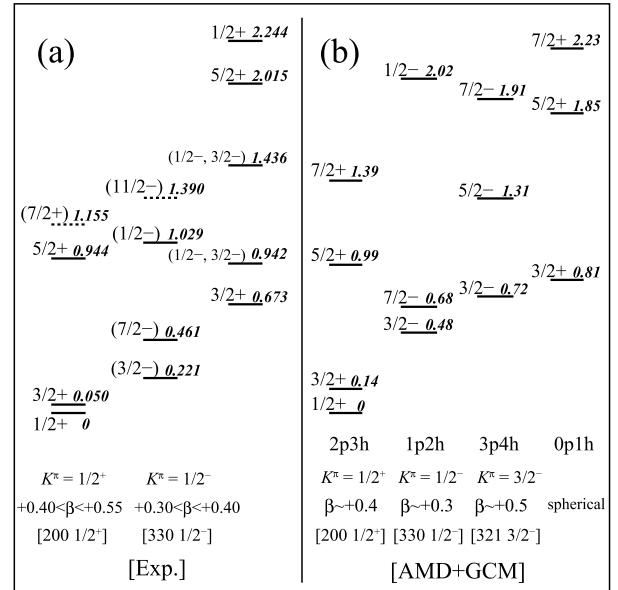


Fig. 5. Comparison between the ^{31}Mg levels of (a) the experimental results and (b) the AMD+GCM calculations. The dominant configurations are shown in the shell model picture, such as $2p3h$, $1p2h$, $3p4h$, and $0p1h$, with notation relative to the $N = 20$ shell closure.

are known in the higher energy region of ^{25}Mg with decoupling parameters $a = -0.5$ and -3.5 , respectively [42]. Since the decoupling parameter is sensitive to the orbit occupied by the unpaired neutron, the closeness of the decoupling parameters in ^{31}Mg and ^{25}Mg suggests the same orbits in the Nilsson diagram. Therefore, we propose that the positive-parity levels [$1/2^+ 0$ MeV, $3/2^+ 0.050$, $5/2^+ 0.944$, $(7/2^+) 1.155$] and negative-parity levels [$(3/2^-) 0.221$, $(7/2^-) 0.461$, $(1/2^-) 1.029$, $(11/2^-) 1.390$] are members of the $K^\pi = 1/2^+$ and $1/2^-$ rotational bands with the configurations of $[200 1/2^+]$ and $[330 1/2^-]$, respectively.

In order to get more insight into the rotational bands in ^{31}Mg , the configurations of the unpaired neutron are considered based on the neutron single-particle orbits in the Woods-Saxon potential as a function of the deformation parameter β [43]. In the Nilsson diagram, it is suggested that the deformation parameters β are in a range of $+0.40 < \beta < +0.55$ and $+0.30 < \beta < +0.40$, respectively, so that the last neutron occupies the $[200 1/2^+]$ and $[330 1/2^-]$ configurations.

Fig. 5(b) shows the results of the AMD+GCM calculations [15]. The levels with four different shapes are predicted at a similar excitation energy region. It is seen that the experimental levels of the $K^\pi = 1/2^+$ and $K^\pi = 1/2^-$ rotational bands are in good agreement with the AMD+GCM calculations, except for the 1.390-MeV ($11/2^-$) level. Note that both the $[200 1/2^+]$ and $[330 1/2^-]$ configurations and the deformation parameters are reasonably reproduced. The AMD+GCM calculations also predict the $K^\pi = 3/2^-$ rotational band with larger deformation. The experimental 0.942-MeV level is probably the $3/2^-$ level of the band-head of the $K^\pi = 3/2^-$ rotational band. The experimental $3/2_2^+$ level at 0.673 MeV and the $5/2_2^+$ level at 2.015 MeV show good correspondence with predicted spherical levels at 0.81 and 1.85 MeV, respectively, taking into account the level energies, spins and parities, and $\log ft$ values.

In the recent shell model calculations for ^{31}Mg [14], the levels with three different configurations of $0p0h$, $1p1h$, and $2p2h$ (hereafter $0p1h$, $1p2h$, and $2p3h$ with the notation relative to the $N = 20$ shell closure, respectively) are predicted below 1 MeV. The theoretical positive- and negative-parity bands built on the $1/2_1^+$

and the $3/2^-_1$ states are in good agreement with the experimental $K^\pi = 1/2^+$ and $1/2^-$ bands, respectively. The shell model also predicts a $3/2^+$ level with the $0p1h$ configuration at ~ 0.4 MeV, and this level shows a good correspondence with the experimental $3/2^+$ level. The AMD+GCM calculations also predict a spherical nature for this level.

The 2.244-MeV $1/2^+$ level with the large β -branching ratio cannot be explained by the AMD+GCM calculations. The large β -branching ratio indicates a large overlap of the wave functions between the 2.244-MeV level and the ground state of ^{31}Na , which is largely deformed [37]. Thus the 2.244-MeV level must have a large collectivity. Also, it is found that the γ -transition intensity from this level to the 0.673-MeV $3/2^+$ level with a spherical configuration is much smaller than that to the ground state $1/2^+$ or the 0.050-MeV $3/2^+$ level with deformed shapes. These facts strongly suggest that the 2.244-MeV level has a large collectivity and has a similar configuration to those of $1/2^+_1$ and $3/2^+_1$ states. A new theoretical approach is awaited to explain this $1/2^+_2$ state at 2.244 MeV.

In summary, the β -delayed γ spectroscopy of spin-polarized ^{31}Na has been very successful in firmly assigning the spins and parities of most of the ^{31}Mg states below the neutron threshold and in revealing very detailed spectroscopic information. By comparing experimental properties of each state with the AMD+GCM calculations on a level-by-level basis, clear evidence was obtained for shape coexistence in the low excitation energy region of ^{31}Mg , such as 7 states which are the members of three types of largely deformed rotational bands and two states with a spherical nature. The 2.244-MeV $1/2^+$ level with a very small $\log ft$ value cannot be explained by theoretical models at present. The present work demonstrates that the β -delayed decay spectroscopy using spin-polarized radioactive beam is a very promising means to explore the shape coexistence in a wide region of the nuclear chart.

Acknowledgements

The authors gratefully acknowledge the staff of TRIUMF for their support and encouragement. This work was supported by JSPS KAKENHI Grants of JP25247039 and JP15H03659. H.N. was supported by a Grant-in-Aid by the JSPS. TRIUMF receives fed-

eral funding via a contribution agreement through the National Research Council of Canada.

References

- [1] B.H. Wildenthal, et al., Phys. Rev. C 22 (1980) 2260(R).
- [2] N.A. Orr, et al., Phys. Lett. B 258 (1991) 29.
- [3] C. Thibault, et al., Phys. Rev. C 12 (1975) 644.
- [4] C. Détraz, et al., Nucl. Phys. A 394 (1983) 378.
- [5] C. Détraz, et al., Phys. Rev. C 19 (1979) 164.
- [6] H. Iwasaki, et al., Phys. Lett. B 522 (2001) 227.
- [7] Y. Yanagisawa, et al., Phys. Lett. B 566 (2003) 84.
- [8] T. Motobayashi, et al., Phys. Lett. B 346 (1995) 9.
- [9] J.A. Church, et al., Phys. Rev. C 72 (2005) 054302.
- [10] A. Watt, et al., J. Phys. G 7 (1981) L145.
- [11] A. Poves, et al., Phys. Lett. B 184 (1987) 311.
- [12] E.K. Warburton, et al., Phys. Rev. C 41 (1990) 1147.
- [13] O. Sorlin, et al., Prog. Part. Nucl. Phys. 61 (2008) 602.
- [14] E. Caurier, et al., Phys. Rev. C 90 (2014) 014302.
- [15] M. Kimura, Phys. Rev. C 75 (2007) 041302(R).
- [16] M. Kimura, Int. J. Mod. Phys. E 20 (2011) 893.
- [17] Focus issue on the shape coexistence in nuclei, J. Phys. G 43 (2) (2016).
- [18] R.F. Casten, Nat. Phys. 2 (2006) 811.
- [19] T. Togashi, et al., Phys. Rev. Lett. 117 (2016) 172502.
- [20] G. Neyens, et al., Phys. Rev. Lett. 94 (2005) 022501.
- [21] G. Klotz, et al., Phys. Rev. C 47 (1993) 2502.
- [22] D. Guillemaud-Mueller, et al., Nucl. Phys. A 426 (1984) 37.
- [23] H. Mach, et al., Eur. Phys. J. A 25 (s01) (2005) 105.
- [24] C.M. Mattoon, et al., Phys. Rev. C 75 (2007) 017302.
- [25] S. Nummela, et al., Phys. Rev. C 64 (2001) 054313.
- [26] J.R. Terry, et al., Phys. Rev. C 77 (2008) 014316.
- [27] D. Miller, et al., Phys. Rev. C 79 (2009) 054306.
- [28] M. Seidlitz, et al., Phys. Lett. B 700 (2011) 181.
- [29] N. Imai, et al., Phys. Rev. C 90 (2014) 011302(R).
- [30] G. Neyens, Phys. Rev. C 84 (2011) 064310.
- [31] G. Neyens, J. Phys. G 43 (2016) 024007.
- [32] C. Ouellet, et al., Nucl. Data Sheets 114 (2013) 209.
- [33] H. Miyatake, et al., Phys. Rev. C 67 (2003) 014306.
- [34] Y. Hirayama, et al., Phys. Lett. B 611 (2005) 239.
- [35] K. Kura, et al., Phys. Rev. C 85 (2012) 034310.
- [36] T. Shimoda, et al., Hyperfine Interact. 225 (2014) 183.
- [37] G. Huber, et al., Phys. Rev. C 18 (1978) 2342.
- [38] C.D.P. Levy, et al., Nucl. Instrum. Methods B 204 (2003) 689.
- [39] C.D.P. Levy, et al., Nucl. Phys. A 746 (2004) 206c.
- [40] C.D.P. Levy, et al., Hyperfine Interact. 225 (2014) 165.
- [41] R.S. Weaver, et al., Nucl. Instrum. Methods 9 (1960) 149.
- [42] A.E. Litherland, et al., Can. J. Phys. 36 (1958) 378.
- [43] I. Hamamoto, Phys. Rev. C 76 (2007) 054319.